Acidoswitchable NLO-phores: Benzimidazolo[2,3-b]oxazolidines

Lionel Sanguinet[†] and Jean-Luc Pozzo*[,†]

Chimie Supramoléculaire, Biomimétisme et Nanoscience, UMR 5802 CNRS, Cours de la Libération, 351, F-33405 Talence Cedex, France

Maxime Guillaume[‡] and Benoît Champagne[‡]

Laboratoire de Chimie Théorique Appliquée, Facultés Universitaires Notre-Dame de la Paix, rue de Bruxelles, 61, B-5000 Namur, Belgium

Frédéric Castet,*[,§] Laurent Ducasse,[§] Etienne Maury,[§] Jérémy Soulié,[§] Fabien Mançois,[§] Frédéric Adamietz,[§] and Vincent Rodriguez*[,§]

Laboratoire de Physico-Chimie Moléculaire, UMR 5803 CNRS, Université Bordeaux I, Cours de la Libération, 351, F-33405 Talence Cedex, France

Received: February 8, 2006; In Final Form: March 30, 2006

This paper presents a series of acidoswitchable NLO-phores combining the 9-methylbenzimidazolo[2,3-*b*]-oxazolidine core with various π systems such as phenylethenyl, phenylethynyl, and naphthylethenyl. All the prepared derivatives are shown to display acidochromic behavior at ambient temperature. The remarkable contrast in the NLO response along the reversible transformations observed in HRS experiments is rationalized by high level theoretical calculations.

1. Introduction

The current interest in miniaturizing the components of electronics down to the molecular level is a major driving force in the research of molecular systems with switchable properties.[1] Among the molecular properties that could be tuned along with this transformation, nonlinear optical (NLO) properties have motivated numerous groups.[2] Systems of interest to display substantial variations of the NLO responses include organic acidochromes/photochromes, which exhibit a large change in electronic distribution between the two states.[3] In fact, acidochromic compounds are characterized by their ability to alternate between two distinct chemical forms having different absorption spectra in response to pH variations whereas in photochromic compounds the transformation between species having different absorption spectra is induced by electromagnetic irradiation.[4] Thus, for instance, one could expect a pronounced change in the first hyperpolarizability (β) for acidochromic or photochromic compounds alternating between a neutral colorless form and a charged colored form. The design of such molecule-based switching devices is directly linked to a number of chemical applications encompassing authentication systems, optical information storage, optical power-limiting substances, and photoresponsive materials, as well as biosensors.

Following the recent report on the synthesis and the NLO properties of a series of acidochromes/photochromes based on the indolino[2,1-*b*]oxazolidine moiety,[5] this paper discusses the synthesis and the NLO properties of a series of acidochromes based on the benzimidazolo[2,3-*b*]oxazolidines moiety (Scheme 1). Our approach in the design of multiaddressable chromophores that could exhibit interesting photo- and/or acidotunable NLO properties is thus based on cyanine dye derivatives, which can present a pure zwitterionic character. Reference 5 demonstrates that the 10-(2-arylethenyl)indolino[2,1-*b*]oxazolidine unit combined with various styrylic residues presents a large contrast of NLO responses along the multiaddressable reversible transformations. In these systems, the basic switching process is associated with the breaking of a σ-bond of the closed form (CF). It is induced either by irradiation to form a zwitterionic species (OF, open form) or by protonation to obtain a colored protonated open form (POF). The present work investigates the structure−property relationships for this family of oxazolidines-based compounds in view of designing systems presenting a large NLO contrast. In particular, the indolino unit of ref 5 is replaced by a benzimidazolo unit whereas acetylenic and ethylenic bridges between the aromatic moieties are compared. This enables to assess the effects of electron conjugation as well as of donor/acceptor strength in a spirit analogous to previous investigations of NLO-phores.[6] In this study, the switch between the open and closed forms is activated by the pH only.

To characterize the electronic as well as linear and nonlinear optical properties of the selected benzimidazolooxazolidines, linear and quadratic nonlinear optical measurements (hyper-Rayleigh scattering: HRS) have been combined with quantum chemical simulations. HRS is known to be the most appropriate method for determining the second-order NLO responses of charged species.[7] On the other hand, theoretical simulations help in interpreting structure−property relationships[8] so that the

* Corresponding authors. E-mail: (V.R.) v.rodriguez@lpcm.u-bordeaux1.fr (NLO measurements); (J.L.P.) jl.pozzo@lcoo.u-bordeaux1.fr (Synthesis); (F.C.) f.castet@lpcm.u-bordeaux1.fr (Calculations).

[†] Chimie Supramoléculaire, Biomimétisme et Nanoscience, UMR 5802 CNRS.

[‡] Laboratoire de Chimie Théorique Appliquée, Facultés Universitaires Notre-Dame de la Paix.

[§] Laboratoire de Physico-Chimie Moléculaire, UMR 5803 CNRS, Université Bordeaux I.

10.1021/jp060825g CCC: $33.50
Published on Web 05/17/2006

SCHEME 1

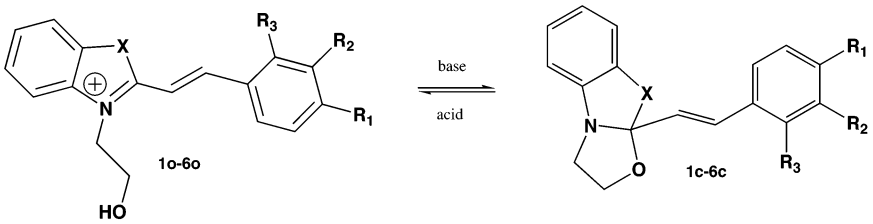

1o X = CMe_2, $R_1 = R_2 = R_3 = H$
2o X = CMe_2, $R_1 = NMe_2$, $R_2 = R_3 = H$
3o X = CMe_2, $R_1 = NMe_2$, R_2-$R_3 = (CH)_4$
4o X = NMe, $R_1 = R_2 = R_3 = H$
5o X = NMe, $R_1 = NMe_2$, $R_2 = R_3 = H$
6o X = NMe, $R_1 = NMe_2$, R_2-$R_3 = (CH)_4$

1c X = CMe_2, $R_1 = R_2 = R_3 = H$
2c X = CMe_2, $R_1 = NMe_2$, $R_2 = R_3 = H$
3c X = CMe_2, $R_1 = NMe_2$, R_2-$R_3 = (CH)_4$
4c X = NMe, $R_1 = R_2 = R_3 = H$
5c X = NMe, $R_1 = NMe_2$, $R_2 = R_3 = H$
6c X = NMe, $R_1 = NMe_2$, R_2-$R_3 = (CH)_4$

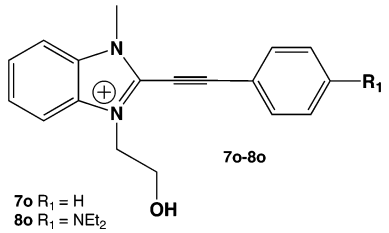

7o $R_1 = H$
8o $R_1 = NEt_2$

SCHEME 2. Synthesis of Target Molecules[a]

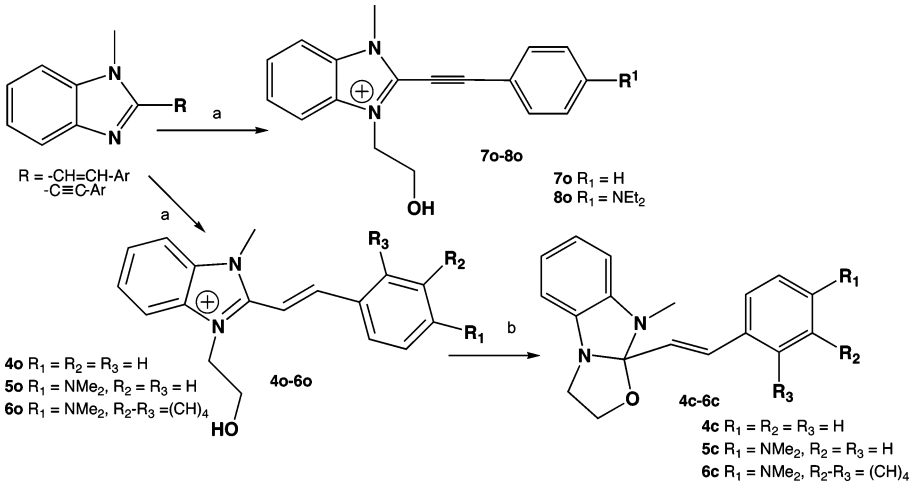

7o $R_1 = H$
8o $R_1 = NEt_2$

4o $R_1 = R_2 = R_3 = H$
5o $R_1 = NMe_2$, $R_2 = R_3 = H$
6o $R_1 = NMe_2$, R_2-$R_3 = (CH)_4$

4c $R_1 = R_2 = R_3 = H$
5c $R_1 = NMe_2$, $R_2 = R_3 = H$
6c $R_1 = NMe_2$, R_2-$R_3 = (CH)_4$

[a] Reagents: (a) 2-iodoethanol; (b) sodium hydride.

mixed theory/experiment analysis is expected to be useful for rational design of new multiaddressable NLO-phores.

2. Synthesis and Characterization

2.1. Synthesis. 10-(2-Arylethenyl)-9-methylbenzimidazolo-[2,3-*b*]oxazolidines **4**−**6c** were synthesized in a two-steps procedure (Scheme 2) starting from various 2-(2-arylethenyl)-1-methylbenzimidazoles which were first reacted with 2-iodoethanol to afford benzimidazolium **4**−**6o**, the latter ones being subsequently converted into benzimidazolo[2,3-*b*]oxazolidines upon basic treatment using sodium hydride. A similar strategic approach was used to prepare compounds **7o** and **8o** incorporating a 2-arylethynyl as substituent in position 2. The quaternarization was achieved in 50−85% yield (see Experimental Section for experimental procedure and spectroscopic data).

2.2. Hyper-Rayleigh Scattering Experiments. All the compounds were prepared as dilute solutions (ranging from 10^{-6} to 10^{-3} mol/L) in acetonitrile, which has a hyper-Rayleigh scattering (HRS) signal for all polarization geometries. Acetonitrile was obtained from Aldrich with a purity of 99.9% (HPCL grade). Solutions were filtered through a 0.2 μm micropore filter to remove dust particles that could be a source of spurious scattered light. Solutions were quantitatively controlled by UV−visible absorption measurements to fulfill accurately linear Beer−Lambert's law. A 90° geometry has been used to record hyper-Rayleigh responses of the samples using a 1064 nm Q-switched Nd:YAG laser (Spectra-Physics). Experimental details have been described elsewhere.[5] Each spectrum was obtained by averaging at least two spectra with an integrating time of 2−20 s, depending on the experimental conditions. All polarized spectra were recorded at room temperature, in conditions where the quadratic dependence of the integrated hyper-Rayleigh scattering intensity is verified.

The second harmonic light intensity for a collection of N noninteracting molecules without orientational correlation (pure incoherent signal) is given by $I^{2\omega} \propto N\langle\mu_i(2\omega)\mu_i^*(2\omega)\rangle$, where the brackets indicate averaging over all possible molecular orientations. The ensemble averaging over the molecular mo-

tions indicated by the brackets will involve products of components of the first hyperpolarizability tensor β of the form $\langle\beta_{IJK}\beta_{LMN}\rangle$. For all the chromophores under investigation, assuming a pseudo C_{2v} molecular symmetry where the molecule lays in a mean (xz) plane, where z is the 2-fold symmetry axis, and assuming Kleinman's conditions, partially justified here because of the strong dipolar nature of the acidochromes (namely the open protonated forms), there are two independent coefficients, which implies here $\beta_{zyy} = \beta_{yyz} = 0$, $\beta_{zxx} = \beta_{xxz} \neq 0$, and $\beta_{zzz} \neq 0$. An accurate setting modulates elliptically polarized incident light (when putting a quarter wave plate after a half wave plate), providing then a phase retardation $\delta = \pi/2$ and a state of polarization characterized by ψ[9]. Circularly polarized left and right lights are described by $\psi = \pm\pi/4$ whereas linearly polarized lights are described by $\psi = 0$ (horizontal H) or $\psi = \pi/2$ (vertical V) giving then the standard HV and VV scattering geometries, respectively. Under these assumptions, for an elliptically polarized incident light, the macroscopic averages $\langle\beta_{IJK}\beta_{LMN}\rangle$ that determine the amount of HRS scattering are

$$I_{\psi V}^{2\omega} \propto \frac{1}{105}\beta_{zzz}^{2}\,[(15 + 18R + 27R^2) - (24 + 60R + 4R^2)\cos^2\psi + (12 + 40R - 12R^2)\cos^4\psi] \quad (1)$$

where $R = \beta_{zxx}/\beta_{zzz}$. Equation 1 implies that a rotation of ψ of the plane of polarization of the fundamental light introduces a quartic dependence in cos ψ which is relevant to determine precisely, within the experimental error, the two independent coefficients β_{zzz} and β_{zxx}.

It is known, for a single molecule, that the HRS light intensity, $I^{2\omega}$, is proportional to the square of the incident light, I^{ω}, and the hyperpolarizability, β. For a two component chromophore-solvent system, the polarized total harmonic scattered light in the VV geometry, $I_{VV}{}^{2\omega}$, is given as the sum of each composition

$$I_{VV}^{2\omega} = G(I^{\omega})^2 B = G(I^{\omega})^2\{[N^{s}\langle(\beta_{ZZZ}{}^{s})^2\rangle + N^{c}\langle(\beta_{ZZZ}{}^{c})^2\rangle]10^{-\alpha^{2\omega}N^{c}}\} \quad (2)$$

where G is a constant, containing theoretical, geometrical, and electrical factors, N is the number density of the solution components (superscript: **s** for solvent and **c** for chromophore), the product term, $\alpha^{2\omega}N^{c}$, accounts for the absorption losses at the second harmonic wavelength (532 nm). From the VV scattering geometry, the determination of the absolute β values of the chromophores is obtained with respect to the response of acetonitrile taken as an internal reference. At low concentrations of the chromophore (solute), where the number density of the solvent, N^{s}, is assumed to be constant, it is shown from eq 2 that $I_{VV}{}^{2\omega}/(I^{\omega})^2$ is a linear function of the number density of the solute, N^{c}, and that $I_{VV}{}^{2\omega}/B$ is a quadratic function of the incident intensity, I^{ω}. A three-dimensional analysis ($I^{2\omega}$, I^{ω}, N^{c}) is then performed, which gives the best physical correlation as illustrated in Figure 1

2.3. Theoretical Details. The molecular structures were fully optimized at the B3LYP/6-311G* level using the Gaussian98 package.[10] The excitation energies ΔE_{ge} and excited-state properties of the chromophores were determined using the CIS (configuration interaction/singles) scheme based on Zerner's INDO (intermediate neglect of diatomic overlap) Hamiltonian[11] available in the MOS−F program.[12] In addition to its applicability to large molecules, the CIS method associated with semiempirical Hamiltonians has been shown to yield accurate predictions of transition energies because, on one hand, most of the low-lying excitations are dominated by single excitations and,

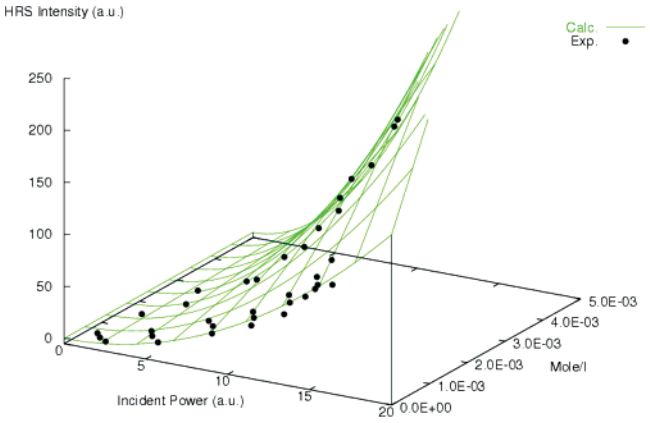

Figure 1. Experimental (points) and best fitted curves (lines) of harmonic light, following eq 2 as a function of the incident power and concentration (in mol/L) of **5o** with irradiation at 1064 nm.

on the other hand, the parameters defining such Hamiltonians are fitted to spectroscopic data.[13] The CIS/INDO/S approach also provides the transition dipole moments between the ground and excited states, $\mu_{ge} = \langle 0|\hat{\mu}|e\rangle$ where $\hat{\mu}$ is the dipole moment operator, the excited-state dipole moments, $\mu_{ee} = \langle e|\hat{\mu}|e\rangle$, as well as the oscillator strengths, $f_{ge} = {}^{2}/_{3}\Delta E_{ge}\mu_{ge}{}^{2}$, which are proportional to the transition probability and absorption intensity. Mulliken population analysis is used to characterize the charge distributions in the ground and excited states, and, therefore, the charge reorganization accompanying the electronic excitations. In all calculations, the complete set of occupied and unoccupied molecular orbitals has been included in the CIS expansions. Subsequently, the hyperpolarizabilities were evaluated using the summation-over-states (SOS) perturbation approach combined with the INDO/S Hamiltonian. Although the SOS scheme is known to overestimate the β values, it has the advantage of expressing the NLO responses in terms of spectroscopic quantities and of providing a qualitative understanding of the NLO properties. This method has been widely popularized by Brédas,[14] Morley,[15] Ratner,[16] and their coworkers for deducing structure−property relationships in a large range of conjugated molecules. Within this approach, the expression of the first hyperpolarizability components reads

$$\beta_{ijk}(-\omega_{\sigma};\omega_1,\omega_2) = \frac{1}{2}\sum P_{-\sigma,1,2}\sum_{n\neq g}\sum_{m\neq g}\frac{\mu_{gn}^{i}\,\bar{\mu}_{nm}^{j}\,\mu_{mg}^{k}}{(\Delta E_{gn} - \omega_{\sigma})(\Delta E_{gm} - \omega_2)} \quad (3)$$

where the sums run over all excited states $|n\rangle$ and $|m\rangle$ of energy E_n and E_m. $|g\rangle$ is the ground-state wave function of energy E_0. $\bar{\mu}_{mn}{}^{j} = \langle m|\hat{\mu}_j|n\rangle - \delta_{mn}\langle g|\hat{\mu}_j|g\rangle$ and $\Delta E_{gn} = \hbar\omega_{gn} = \omega_{gn} = E_n - E_g$. $\Sigma P_{-\sigma,1,2}$ is the sum over the six permutations of the pairs $(-\omega_{\sigma}, i)$, (ω_1, j), and (ω_2, k). Within the two-states approximation, the diagonal components of the SHG response reduce to

$$\beta(-2\omega;\omega,\omega) = 3\mu_{ge}{}^{2}\,\bar{\mu}_{ee}\frac{\Delta E^2}{(\Delta E^2 - 4\omega^2)(\Delta E^2 - \omega^2)} = \beta_0\frac{\Delta E^4}{(\Delta E^2 - 4\omega^2)(\Delta E^2 - \omega^2)} \quad (4)$$

All SOS calculations of β were performed using the MOS−F program by including the whole set of excited states in the summations. The NLO properties of the chromophores were also computed at other semiempirical and ab initio levels using analytical and numerical derivatives formalisms. First, the time-

dependent Hartree−Fock (TDHF) scheme and, for static quantities, the coupled-perturbed Hartree−Fock (CPHF) methods have been employed. These schemes consist in expanding the matrices of the TDHF/CPHF equations in Taylor series of the external (static and/or dynamic) electric field and in solving these analytically order by order.[17] To get the first hyperpolarizability tensor, only first-order derivatives of the LCAO coefficients are needed, provided the $2n + 1$ rule is employed to express it. The TDHF and CPHF schemes were employed using the 6-31G, 6-31G*, and 6-31+G* basis sets. CPHF calculations were also performed in combination with the semiempirical AM1,[18] PM3,[19] and PM5 [20] Hamiltonians. To our knowledge, this investigation reports the first assessment of the CPHF/PM5 scheme for computing the first hyperpolarizability of D/A compounds in comparison with other semiempirical and ab initio approaches. Often, these approximations make it possible to study large conjugated compounds within reduced calculation times while reproducing fairly well the quality of ab initio correlated methods.[21] The semiempirical CPHF calculations were carried out using the MOPAC package [22] whereas GAUSSIAN03[10] was used for the ab initio part. In the ab initio calculations, electron correlation effects were then included using the second-order Møller−Plesset (MP2) method and the finite field (FF) procedure.[23] The field-dependent energies were determined using Gaussian03 in combination with the iterative Romberg procedure to improve the accuracy on the differentiation procedures.[24] The numerical accuracy is on the order of 1.0 au or less as determined from comparing the equivalent HF/FF and CPHF results. Frequency dispersion effects were estimated at the MP2 level by adopting the percentage or multiplicative correction scheme[25]

$$\beta_{\mathrm{MP2}}(-2\omega;\omega,\omega) \approx \beta_{\mathrm{MP2}}(0;0,0) \times \frac{\beta_{\mathrm{TDHF}}(-2\omega;\omega,\omega)}{\beta_{\mathrm{CPHF}}(0;0,0)} \quad (5)$$

which has been shown to be suitable for different systems including push−pull polyenes. No density functional theory (DFT) approaches were used for determining the NLO responses since conventional DFT schemes fails drastically while the optimized effective potential procedure for exact exchange (OEP-EXX) still requires to be combined with a suitable correlation functional.[26] All first hyperpolarizability values are consistent with convention B of ref 27. Full expressions without assuming Kleinman's conditions have been used to determine the HRS responses.[28]

3. Experimental Results

The molecules have been designed to display various donor/acceptor and electron conjugation characters. Within the series, a strong electrondonating group *N*,*N*-dimethylamino was introduced onto the aryl moieties. By replacing the phenyl moiety by a naphthyl group (**6o**) the impact of the nature of the aromatic ring has been addressed. Finally, the effect of the nature of the bridge is considered by replacing the ethylenic group in **4o**−**5o** by an acetylenic bridge **7o**−**8o**. All prepared compounds have been compared with the protonated open forms **1o**−**3o** of the corresponding indolinooxazolidines **1c**−**3c**, which have been shown to exhibit substantial NLO contrast upon acidic changes.

3.1. Linear Optical Properties. The CFs are very sensitive to the presence of proton since a slight addition of ethanol or of chlorhydric acid stabilizes the OP as reported in Figure 2. Reversibly, as schemed in section 2.1, addition of sodium hydride switches the colored form toward the uncolored one.

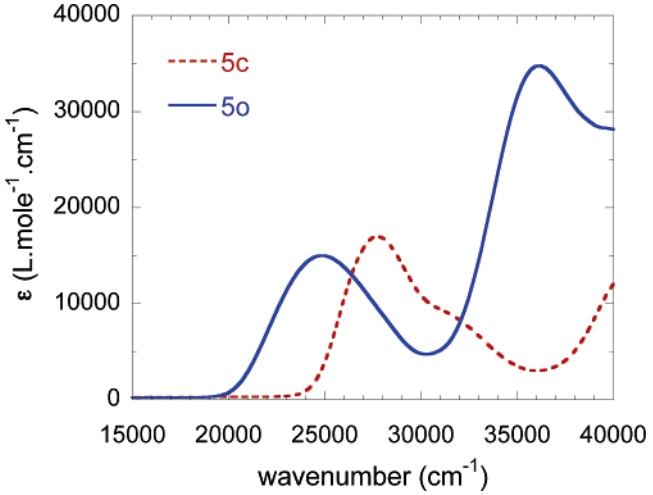

Figure 2. UV−visible absorption spectra of **5c** and **5o** obtained upon addition of HCl.

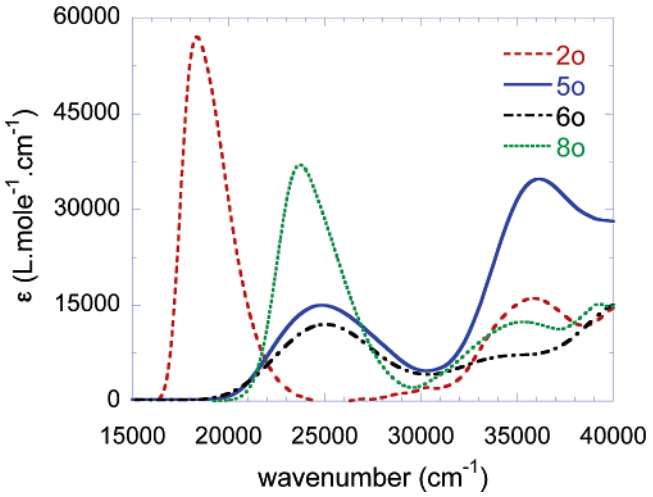

Figure 3. UV−visible absorption spectra of **2o**, **5o**, **6o**, and **8o**.

In contrast to the indolinooxazolidine family studied previously,[5] in the benzimidazolo series, the difference between the absorption spectra of the closed and open forms is less pronounced, both in terms of excitation energies and of oscillator strength. Figure 3 displays the absorption spectra of the colored forms. All maxima of absorption range between ∼24000 cm^{-1} (422 nm for **8o**) and ∼25000 cm^{-1} (402 and 406 nm for **5o** and **6o**, respectively. In the visible range (15000−30000 cm^{-1}), the spectra of the benzyl (**5o**) and naphthyl (**6o**) derivatives are very similar, whereas in the indolino series, λ_{max} of **2o** and **3o** differ by as much as 29 nm.[5] Besides, the absorption maximum of **8o** containing a CC triple bond occurs at slightly lower energy than for the **5o** or **6o** compounds having an ethylenic bridge. This peculiar point is discussed hereafter in the theoretical section. The absorption cross sections of **5o** and **6o** are comparable but only half of **8o** and roughly one-third of **2o**, which is representative of the indolinooxazolidine series.

3.2. NLO Properties. The molecular hyperpolarizabilities, β_{zzz} and β_{zxx}, have been determined for all compounds and the results are reported in Table 1. The obtained values are listed in atomic units (au) and were measured at 1064 nm in acetonitrile. Static β values (β_0) have been obtained by extrapolating the dynamic quantities using the two-state approximation and eq 4. Taking chromophores **5c**/**5o** as an illustration, Figure 4 details the quadratic power dependence of the scattered harmonic light for several chromophore

TABLE 1: Linear and Nonlinear Optical Properties of Selected Chromophores at 1064 nm[a]

	λ_{max} (nm)	β_{zzz}^{1064} (au)	β_{zzz}^{1064} (10^{-40} m^4/V)	R	$I_{VV}^{2\omega}/I_{HV}^{2\omega}$	β_0 (au)	β_0 (10^{-40} m^4/V)	$\tau_{o/c}$ (%)
2o	544	144000 ± 6000	5213	−0.006 ± 0.013	4.94 ± 0.05	4850	176	97
5o	402	27500 ± 3000	946	+0.052 ± 0.014	5.47 ± 0.05	10100	366	81
6o	406	13600 ± 3000	492	−0.046 ± 0.030	4.57 ± 0.08	5000	181	83
8o	422	95000 ± 6000	3439	+0.001 ± 0.005	5.01 ± 0.02	29600	1072	

[a]The absorption maximum is given by λ_{max} (nm). Absolute values of the longitudinal hyperpolarizability, β_{zzz}^{1064} are given in atomic and MKS units (1 au = 3.6213×10^{-42} m^4 V^{-1} = 3.206361×10^{-53} C^3 m^3 J^{-2} = 8.6392×10^{-33} esu). The static hyperpolarizability, β_0 (β_{zzz}^{∞}), is estimated from the two-states model. The normalized efficiency of the longitudinal hyperpolarizability contrasts between the POF and CF are defined as $\tau_{O/C}$ = $[\beta_{zzz}^{1064}((POF) - \beta_{zzz}^{1064}(CF)]/\beta_{zzz}^{1064}(POF)$. Chromophore **2o** (indexed as **4d** in ref 5) results are included for comparison purposes.

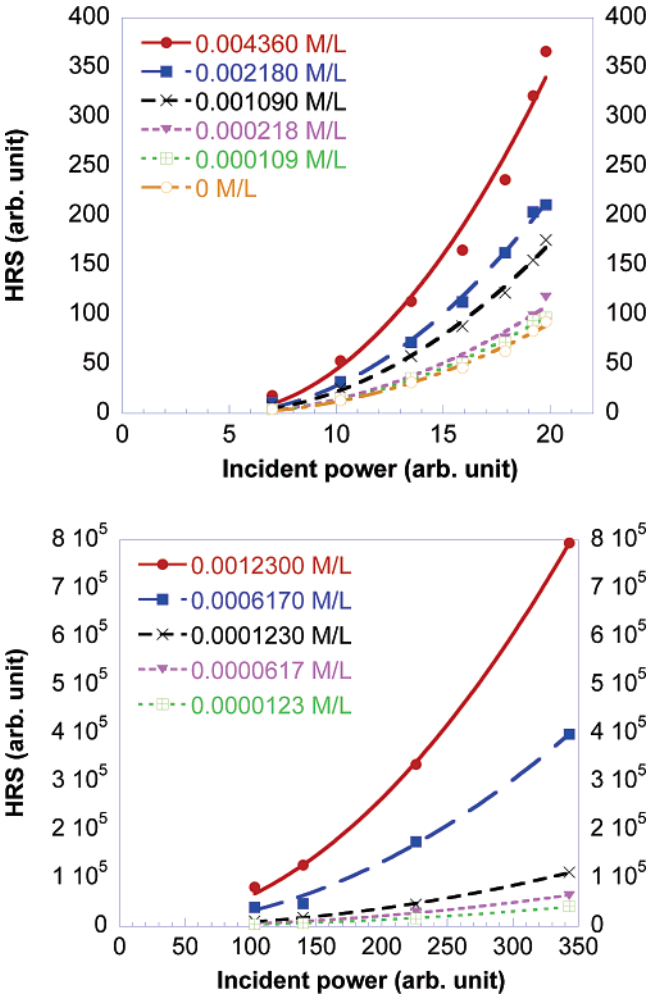

Figure 4. Experimental (points) and best fitted curves (lines) of harmonic light intensity, following eq 2, as a function of the incident power and concentration (in mol/L) of **5c** (top) and **5o** (bottom) with irradiation at 1064 nm.

concentrations. Figure 5 gives a typical polar plot of the obtained polarization ratios $I_{\psi V}^{2\omega}/I_{HV}^{2\omega}$ with the retardation angle ψ for a protonated compound. For this compound, **8o**, we find a polarization ratio $I_{VV}^{2\omega}/I_{HV}^{2\omega}$ = 5.01 (Table 1) very close to the value of the pure rodlike dipole where $I_{VV}^{2\omega}/I_{HV}^{2\omega}$ = 5.

Since the harmonic wave is far from any resonance of **5o**, **6o**, and **8o**, all their dynamic longitudinal values, β_{zzz}^{1064} are below the indolinooxazolidine derivative **2o** response. The dynamic hyperpolarizabilities of the ethylenic bridge derivatives, **5o** and **6o**, are roughly 1 order of magnitude smaller than that of **2o**. The large difference observed between both the dynamic and static extrapolated responses of **5o** and **6o** cannot be explained by the differences of position (4 nm) or absorption cross-section (12 000 vs 15 000 L mol^{-1} cm^{-1} for **6o** and **5o**, respectively) of the first dipole-allowed transition. However, it

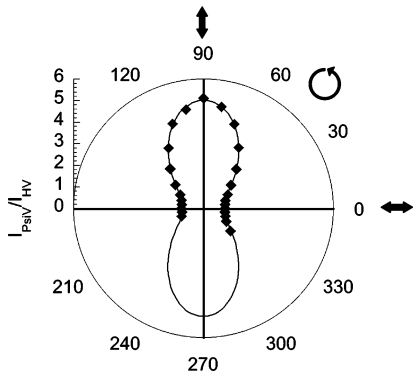

Figure 5. Polar plot of the measured (solid squares) and calculated (solid line) polarization ratios, $I_{\psi V}^{2\omega}/I_{HV}^{2\omega}$, of **8o** with irradiation at 1064 nm, as a function of the retardation angle ψ (in degrees). The curve shows that the HRS polarization data can be well fitted assuming **8o** has a pseudo planar C_{2v} symmetry with $R = \beta_{zxx}^{1064}/\beta_{zzz}^{1064}$ = +0.001 ± 0.005.

could be related to the presence in the linear absorption spectrum of **5o** of an intense transition at higher energy (Figure 3). The larger β values of **8o** with respect to **5o** and **6o** are consistent with the larger oscillator strength of the first absorption band. β of **8o** is also very large, considering the fact it attains 50% of the **2o** β value whereas it is not enhanced by resonance. As expected, for all compounds, the minor/major hyperpolarizability ratio R is close to the dipolar value of 5. Finally, the contrast of the dynamical longitudinal hyperpolarizabilities, $\tau_{o/c}$, between the open and closed forms is as high as ~80% for **5o** and **6o**, more representative than **2o** (97%), which is resonantly enhanced.

4. Theoretical Results

The optimized structures of molecules **5**, **6**, and **8** in their POFs are schematized in Figure 6, as well as the closed structures **5c** and **8c**. In **8o**, the extreme NEt_2 group has been replaced by NMe_2 to simplify the calculations. Molecules **5o** and **6o** present a dihedral angle N2−C3−C6−C8 between the planes of the six-membered rings on both sides of the conjugated bridge equal to 45 and 57°, respectively. The corresponding torsion angle in **8o** is smaller and amounts to 17°. Moreover, in **5o** and **6o** there is a hydrogen bonding between the oxygen atom and one of the hydrogens of the bridge, that stabilizes the position of the CH_2CH_2OH chain. In all closed forms **5c** and **8c**, the benzimidazole and the arylethynyl parts are quasi-perpendicular (the dihedral angle N2−C3−C6−C8 amounts to 114 and 116° in **5c** and **8c**, respectively).

4.1. Linear Optical Properties. Since in their CF the chromophores do not present significant NLO responses (vide infra), only the POF forms have been considered for simulations. The transition energies, oscillator strengths, changes in dipole moments, and molecular orbital (MO) characteristics of the most significant charge-transfer excitation of **5o**, **6o**, and **8o** calculated at the INDO/S level are gathered in Table 2.

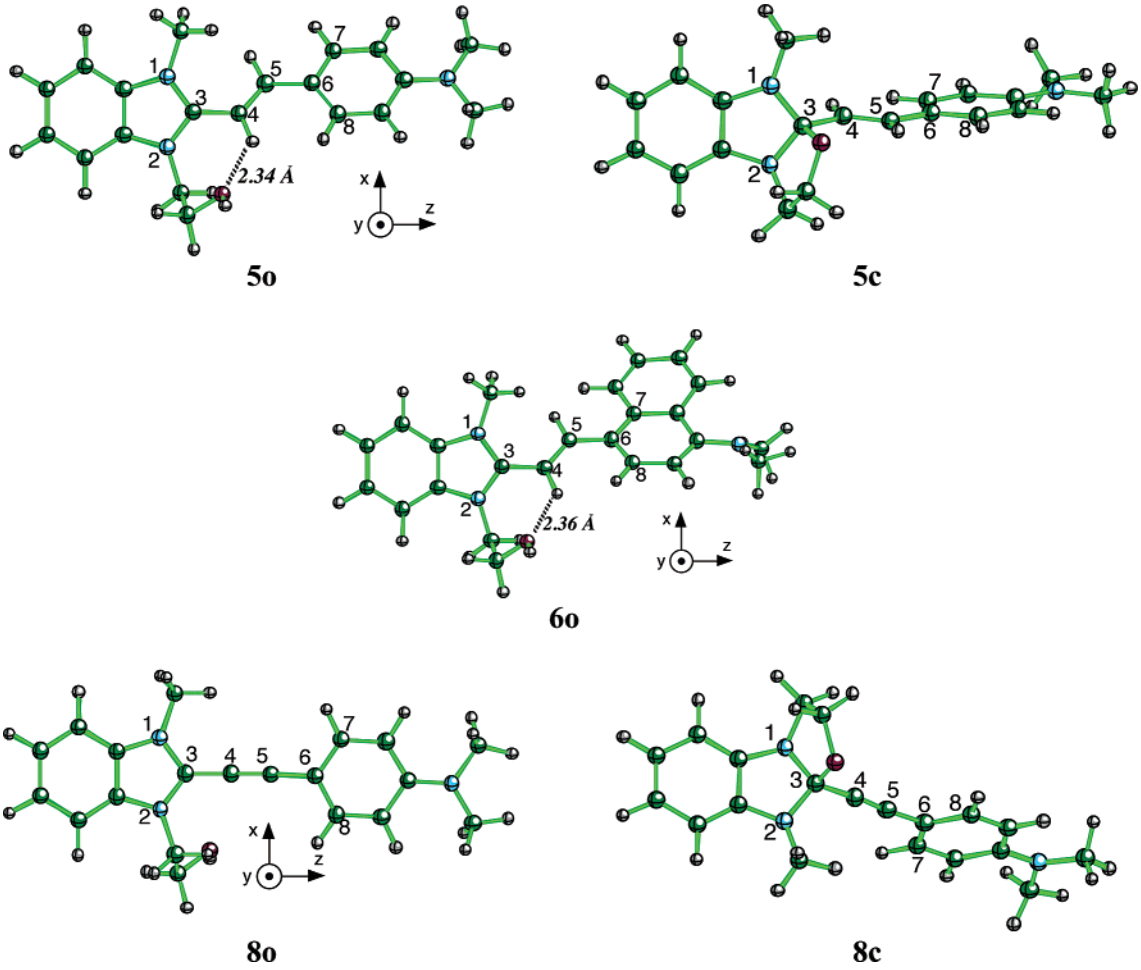

Figure 6. Optimized structures and Cartesian frame used in the theoretical calculations.

TABLE 2: INDO/S Transition Energies (ΔE_{ge}, eV), Wavelengths (λ_{ge}, nm), Oscillator Strengths (f_{ge}), and Dipole Moment Changes ($\Delta\mu_{ge}$, Debye) for the Dominant Low-Energy Charge-Transfer Excited State[a]

	ΔE_{ge}	λ_{ge}	f_{ge}	$\Delta\mu_{ge}$	main CI coeffs
5o	2.67 (3.08)	464 (402)	1.240	9.10	87% H → L
6o	2.42 (3.05)	513 (406)	1.090	8.76	89% H → L
8o	2.70 (2.94)	459 (422)	1.091	8.96	80% H → L +
	2.62[b]	473[b]			6% H-1 → L
2o	2.50 (2.28)	497 (544)	1.405	4.70	91% H → L

[a] The last column reports the main CIS expansion coefficients. H = HOMO; L = LUMO. Experimental ΔE_{ge} and λ_{ge} values are given in parentheses [b] After Maxwell−Boltzmann averaging over the torsion angles.

The most absorbing charge-transfer excited state of the POF is dominated by a $\pi \rightarrow \pi^*$ transition between the highest occupied molecular orbital (HOMO) and the lowest unoccupied molecular orbital (LUMO). The shape of the two orbitals involved in the excitation is quite similar in all the chromophores. As shown in Figure 7 for **5o**, the HOMO is mainly localized on the *N*,*N*-dimethylaminophenyl moiety, while the LUMO is delocalized over the whole system. This rather large difference in the global form of the two orbitals involved in the lowest energy excitation is a first indication of a large electron reorganization under light irradiation, consistent with a substantial change in the dipole moments (Table 2). The efficiency of the charge transfer occurring from the *N*,*N*-dimethylaminophenyl group toward the ethylenic bridge and the benzimidazole group may also be highlighted by analyzing the differences in the Mulliken charge distributions between the ground and the first excited state, as reported in Figure 8. Similarly to the indolino[2,1-*b*]oxazolidine series,[5] the phenyl group of the benzimidazole does not display any significant variation of charge upon excitation. However, the charge transfers and the dipole moment changes are almost twice as large in the benzimidazole series than in the indolino series.

Overall, it is noteworthy that the relative INDO/S values of λ_{ge} seem not consistent, even qualitatively, with the experimental measurements. In particular, although the relative values of oscillator strength are well reproduced, the calculated excitation wavelengths of **5o** and **6o** differ by as much as 49 nm whereas the experimental values are within 4 nm. This small experimental difference also contrasts with the results on the indolino series where the calculated (54 nm) and experimental (29 nm) differences are much consistent. Moreover, the experimental maximum absorption wavelength of **5o** is found to be smaller than the one of **8o** by 20 nm, while calculations predict the reversal hierarchy. Time-dependent density functional (TD-DFT) calculations were then carried out at the B3LYP/6-311G* level to address the reliability of the Zerner's parametrization for our molecular systems, and led to very similar relative transition wavelengths for **5o**, **6o**, and **8o** [$\Delta\lambda$(**5o**/**6o**) and $\Delta\lambda$(**5o**/**8o**) are equal to +49 and −5 nm at the INDO/S level and to +54 and −3 nm within TD-B3LYP/6-311G*].

Beyond the unavoidable solvent effects that might affect the relative transition energies, these discrepancies between experiment and theory might originate from the presence of several conformers in solution, in particular due to the rotation of the electron-donating styryl/tolyl group around the C5−C6 bond. Thus, the potential energy curve along this dihedral angle was

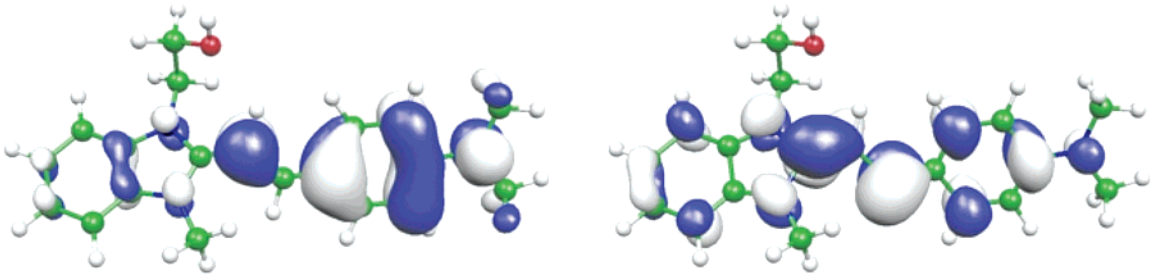

Figure 7. Highest occupied molecular orbital (left) and lowest unoccupied molecular orbital (right) of the **5o** compound.

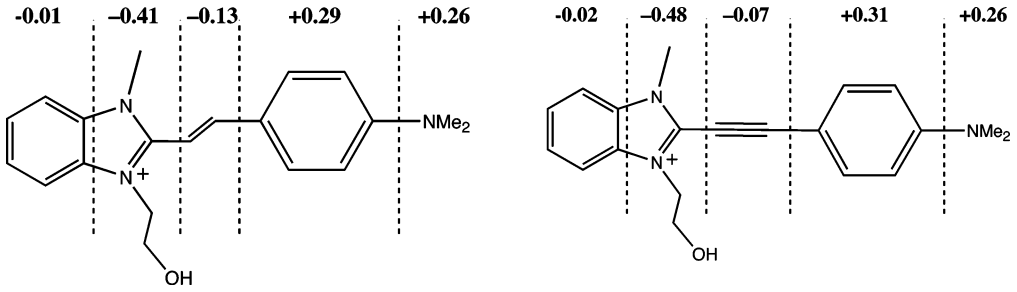

Figure 8. Mulliken charge differences (in electron units) between the ground and the first excited-state calculated at the INDO/S level for the **5o** (left) and the **8o** (right) compounds.

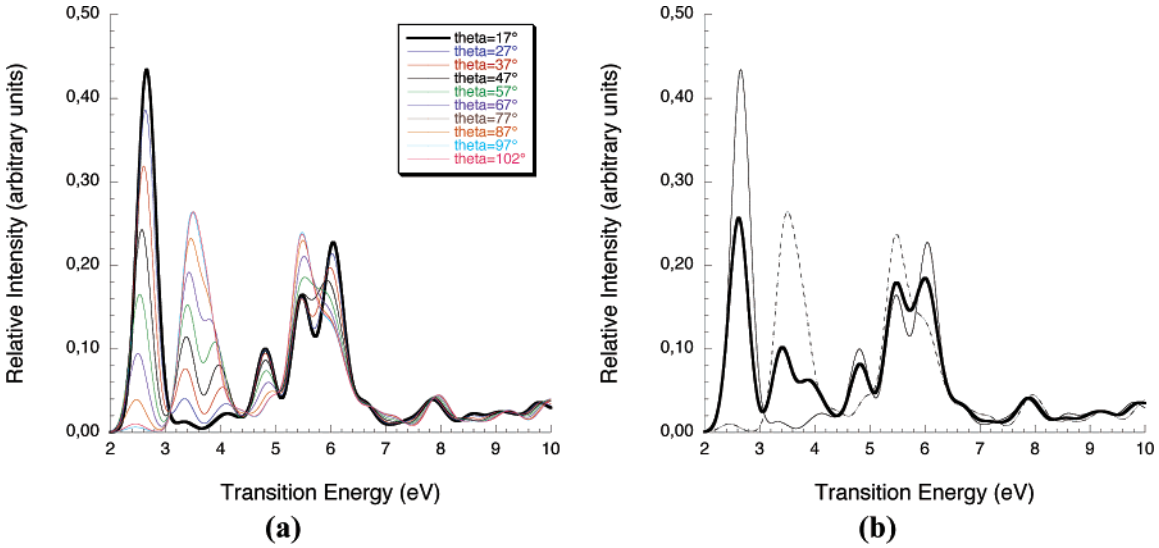

Figure 9. (a) Simulated INDO/S electronic absorption spectrum of **8o** as a function of the torsional angle N2−C3−C6−C8. (b) Spectra of the extreme rotamers and Maxwell−Boltzmann averaged absorption spectrum (bold line).

determined at the semiempirical AM1 level for compounds **5o** and **8o** by varying step by step the value of the dihedral angle N2−C3−C6−C8 (see Figure 6) while all the other structural parameters were reoptimized at each step. For **5o**, the potential energy increases rapidly with the torsion and the rotation barrier reaches 5.5 kcal/mol, so that, at room temperature, only the most stable conformer should exist. On the other hand, the rotational barrier for **8o** is small enough (1 kcal/mol) to include in the simulation of the absorption spectrum more than one rotamer. This large difference is easily understood from comparing the overlap interactions between the π atomic orbitals of the bridge and those of the rotating styryl/tolyl residue in the two chromophores. Indeed, after rotation of the *N*,*N*-dimethylaminophenyl in **5o** by 90°, the orbitals of the two fragments are orthogonal, and the stabilization due to overlap interactions vanishes. On the contrary, the magnitude of the corresponding overlap interactions in **8o** is quasi independent of the orientation of the phenyl group due to the presence of the central triple bond.

Subsequently, the absorption spectrum of **8o** was simulated at the INDO/S level for different values of the torsion angle. The oscillator strengths, which are proportional to the transition probability, are used to evaluate the relative absorption intensities. Each transition is modeled by a Gaussian function with full width at half-maximum (fwhm) of 0.4 eV. The set of spectra reported in Figure 9a clearly shows the impact of structural changes on the absorption properties. An increase in torsion angle gives rise to a bathochromatic shift of the first absorption band associated with a decrease of its intensity. At the same time, a wide 2-components band progressively emerges between 3 and 4.5 eV. Beyond 60°, the latter band becomes the main absorption band, until the complete vanishing of the first low-energy band. To get a better comparison with experiments, an averaged absorption spectrum was simulated where the contributions of the rotamers are weighted according to the Maxwell−Boltzmann distribution. The resulting absorption spectrum is reported in Figure 9b as well as the spectra corresponding to the two extreme torsion angles. The general shape of the mean

TABLE 3: Static Longitudinal First Hyperpolarizability (β_{zzz}), HRS First Hyperpolarizability (β_{HRS}), and Depolarization Ratio (DR) of the Different POF Evaluated at Different Levels of Approximation, Where the β Values Are Given in au and in Parentheses Are Given the Ratios with Respect to 5o

	5o	**8o**	**8o**-45°	**8o**-90°	**6o**	**2o**
			HF/6-31G			
β_{zzz}	5065 (1.000)	5201 (1.027)	4181 (0.825)	1723 (0.340)	5035 (0.994)	5845 (1.154)
β_{HRS}	2097 (1.000)	2117 (1.010)	1699 (0.810)	690 (0.329)	2090 (0.997)	2379 (1.135)
DR	4.53	4.58	4.54	4.12	4.52	4.30
			MP2/6-31G			
β_{zzz}	11666 (1.000)	11697 (1.003)	9064 (0.777)	3494 (0.300)	12972 (1.112)	11983 (1.027)
β_{HRS}	4963 (1.000)	4813 (0.970)	3728 (0.751)	1433 (0.289)	5567 (1.122)	4796 (0.986)
DR	4.85	4.84	4.83	4.70	4.96	4.70
			HF/6-31G*			
β_{zzz}	4707 (1.000)	4813 (1.023)	3887 (0.826)	1571 (0.335)	4642 (0.986)	5385 (1.144)
β_{HRS}	1949 (1.000)	1959 (1.005)	1579 (0.810)	631 (0.324)	1928 (0.989)	2192 (1.125)
DR	4.53	4.57	4.53	4.08	4.50	4.30
			MP2/6-31G*			
β_{zzz}	10376 (1.000)	10421 (1.004)	8203 (0.791)	3152 (0.304)	11520 (1.110)	10070 (0.970)
β_{HRS}	4412 (1.000)	4286 (0.971)	3373 (0.765)	1292 (0.293)	4945 (1.121)	4112 (0.932)
DR	4.85	4.83	4.83	4.68	4.95	4.68
			AM1			
β_{zzz}	12464 (1.000)	10275 (0.824)	8192 (0.657)	4433 (0.356)	13398 (1.075)	14591 (1.170)
β_{HRS}	4749 (1.000)	3806 (0.801)	3024 (0.637)	1616 (0.340)	5160 (1.087)	5368 (1.130)
DR	4.69	4.65	4.60	4.37	4.77	4.54
			PM3			
β_{zzz}	15345 (1.000)	11909 (0.776)	9347 (0.609)	4706 (0.307)	16227 (1.057)	17454 (1.137)
β_{HRS}	5880 (1.000)	4412 (0.750)	3449 (0.587)	1709 (0.291)	6249 (1.063)	6443 (1.096)
DR	4.71	4.65	4.60	4.32	4.81	4.61
			PM5			
β_{zzz}	13319 (1.000)	10210 (0.767)	8387 (0.630)	5350 (0.402)	13584 (1.020)	16006 (1.202)
β_{HRS}	5071 (1.000)	3775 (0.774)	3091 (0.610)	1954 (0.385)	5208 (1.027)	5893 (1.162)
DR	4.69	4.62	4.57	4.41	4.76	4.56
			SOS/INDO/S			
β_{zzz}	14064 (1.000)	14473 (1.029)	11094 (0.789)	2784 (0.198)	15434 (1.097)	14470 (1.029)
β_{HRS}	5223 (1.000)	5305 (1.016)	4051 (0.776)	962 (0.184)	5748 (1.101)	5236 (1.002)
DR	4.37	4.46	4.42	3.52	4.40	4.08

spectrum is now in qualitative agreement with experiment, reported in Figure 3. The corrected value of the maximum absorption wavelength is 473 nm, higher than the value of 464 nm obtained for **5o** at the same level of theory. Although the difference of 9 nm in the relative λ_{max} values of **5o** and **8o** is still underestimated compared to experiment (20 nm), these calculations demonstrate that the electronic properties, and consequently the NLO properties, of **8o** should not be analyzed by considering a unique rotamer.

4.2. Simulation of NLO Properties. Table 3 lists the static longitudinal first hyperpolarizability (β_{zzz}), the HRS first hyperpolarizability (β_{HRS}), and the depolarization ratio (DR) as calculated at different levels of approximations for selected systems. In particular, the ratios with respect to the reference **5o** compound are given. At ab initio levels, as well as at the SOS/INDO/S, **5o** and **8o** present similar β values whereas for the semiempirical AM1, PM3, and PM5 Hamiltonians, the β of the **5o** compound is about 20−25% larger. As expected from section 4.1, when rotating in **8o** the Ph−NMe_2 out of the molecular plane, the dominant β components decrease so that the HRS response is reduced by 20−40% (60−70%) for a dihedral angle of $\pi/4$ ($\pi/2$). The SOS/INDO/S level of calculation predicts a larger decrease of the HRS response (81%) and of the DR. Replacing the phenyl by a naphthyl substituant (**6o** vs **5o**) leads to a slight increase of the first hyperpolarizability (except at the HF/6-31G and HF/6-31G* levels of approximation). A similar conclusion holds for **2o** vs **5o**, i.e. when replacing X = CMe_2 by X = NMe. Besides the reduction of DR accompanying the increase in dihedral angle, little changes of the DR are found among the compounds. In fact, the MP2 DR are larger than their HF analogues, bracketing the semiempirical values.

In most cases, the PM3 method provides the largest static β values among the semiempirical methods whereas AM1 has the smallest. The latter values are also the semiempirical data in closest agreement with the MP2 results obtained using the 6-31G and 6-31G* basis sets. Though basis set effects are not easy to investigate at the MP2 level for compounds of this size, β calculations have also been carried out using the 6-31+G* basis set. Using the 6-31G, 6-31G*, and 6-31+G* basis sets, the β_{HRS} values of **5o** are in the 1.00:0.93:0.98 ratio at the HF level while in the 1.00:0.89:0.94 ratio at the MP2 level, demonstrating weak basis set effects.

Enhanced differences between the second-order NLO responses are observed when accounting for frequency dispersion (Table 4). In particular, at the TDHF level of approximation, **6o** and **2o** present β values about 20% larger than **5o** whereas β is 5% smaller in **8o**. Using the percentage correction scheme (eq 5) with static MP2 values, **6o** turns out to possess the largest β values. At this most elaborated level considered here, **5o** presents larger β responses than **8o** in its equilibrium conformation. Accounting for the ease of rotation of the tolyl moiety, the difference in β between **5o** and **8o** is even larger and can be estimated to reach 10−20% at λ = 1064 nm. **2o** and **5o** present similar β values. SOS/INDO/S calculations give rise to similar conclusions. However, resonance effects encountered in **6o** and **8o** (when rotating the Ph−NMe_2 group by 45°) lead to numerical instabilities in the latter calculations.

TABLE 4: Dynamic (SHG, $\lambda = 1064$ nm) Longitudinal First Hyperpolarizability (β_{zzz}), HRS First Hyperpolarizability (β_{HRS}) of the Different POF Evaluated at Different Levels of Approximation Where the β Values Are Given in au and in Parentheses Are Given the Ratios with Respect to 5O

	5o	**8o**	**8o**-45°	**8o**-90°	**6o**	**2o**
			Equation 5/6-31G			
β_{zzz}	21131 (1.000)	19959 (0.945)	15498 (0.733)	4586 (0.217)	28512 (1.349)	24192 (1.145)
β_{HRS}	9059 (1.000)	8229 (0.908)	6392 (0.706)	1881 (0.208)	12457 (1.375)	9862 (1.089)
			Equation 5/6-31G*			
β_{zzz}	19014 (1.000)	18133 (0.954)	14434 (0.759)	4173 (0.219)	25664 (1.350)	20433 (1.075)
β_{HRS}	8145 (1.000)	7472 (0.917)	5956 (0.731)	1709 (0.210)	11225 (1.378)	8323 (1.022)
			SOS/INDO/S			
β_{zzz}	85227 (1.000)	74579 (0.875)	77421 (0.908)	4477 (0.052)	342166 (4.015)	133825 (1,570)
β_{HRS}	32600 (1.000)	27780 (0.852)	28908 (0.887)	1546 (0.047)	134290 (4.119)	49322 (1.513)

5. Discussion and Concluding Remarks

The experimental β_{zzz}^{1064} value of **5o** (Table 1) is roughly 50% larger than the best theoretical values (Table 4) obtained at the MP2/6-31G* level with inclusion of frequency dispersion through eq 5. On the other hand, for the β_0 quantity, the agreement between theory and experiment is very good, provided electron correlation effects are taken into account. This difference between the quality of the estimates of the static and dynamic values is therefore related to the usual overestimation of the excitation energies at the corresponding RPA level, of which the impact on β increases with the photon energy. Going from **5o** to **8o**, experiment shows a strong enhancement of both β_{zzz}^{1064} (+240%) and β_0 (+190%) whereas theory predicts a decrease by about 10−20%. This cannot be explained by considering the small bathochromatic shift of the main charge-transfer absorption band when going from **5o** to **8o**. On the other hand, this is consistent with the larger oscillator strength in **8o**, which is not reproduced in the theoretical simulations. A possible reason for this discrepancy is the lack of solvent effects in the simulation. At a 1064 nm wavelength, comparison with **2o** is difficult because of the resonance enhancement. However, theory predicts that β_0 of **2o** is of similar amplitude as that of **5o** and **8o** but that its frequency dependence is stronger.

The very small β_{zzz}^{1064} and β_0 values measured for **6o** are not consistent with the excitation energy and oscillator strength for its main CT excited state, which are not much different from that of **5o** (Table 2). The hydrogen bridge between the alcohol group and the solvent acetonitrile may be a possible explanation for this inconsistency. However, such an effect was not observed in the previously investigated indolino series. Another plausible explanation is the formation of dimers or small aggregates—more favored in **6o** due to the naphthyl π-stacking than in **5o** with the smaller benzyl ring—of which the dipolar character is reduced with respect to the parent monomers. Dimerization effects and their detrimental impact on the second-order NLO responses were indeed already observed for systems such as merocyanine dyes.[29] This is supported on one hand by variations of the λ_{max} of absorption when varying the concentration down to 10^{-4} mol L^{-1}. On the other hand, theory predicts a smaller excitation energy for **6o** than **5o** whereas the experimental values are similar. This difference can be related to the so-called exciton shift in dimers. Why these aggregation effects would appear in the benzimidazolo series but not in the indolino series remains an open question.

Theory predicts that in the benzimidazolo[2,3-*b*]oxazolidine series the naphthyl derivative (**6o**) displays β values up to 35% larger than their phenyl analogue (**5o**). The difference is mostly due to stronger frequency dispersion in **6o** associated with smaller excitation energies. This substitution effect is larger than in the parent indolino[2,1-*b*]oxazolidine series because in the latter, the compound with the *N*,*N*-dimethylaminophenyl (**2o**) presents a larger β_0 value than its naphthyl analogue (**3o**) while the frequency dispersion is larger in **3o** than in **2o**. Thus, although **2o** presents a larger β value than **5o**, as obtained from comparison with the results of Ref. 5, **6o** displays a larger β value than **3o**. As a consequence, the torsion of the *N*,*N*-dimethylaminophenyl/naphthyl part with respect to the ethylene bridge and the benzimidazolo moiety, which is induced by the methyl group on N1 has a little impact on β. This can partly be related to the fact the conjugation does not extend much in the benzimidazolo moiety.

This study has shown that NLO-phores based on the benzimidazolo[2,3-*b*]oxazolidine moiety exhibit a substantial NLO contrast between the open and closed forms, as a result of pH variations. This opens the way to efficient acidoswitchable NLO compounds. Further investigations will address the effects of chemical substitutions on the acceptor part of the chromophores in order to extend the conjugation path.

6. Experimental Section

General Procedure for the Preparation of 2-(2′-Arylethenyl)-1-(2-hydroxyethyl)-3-methylbenzimidazolium Iodide 4o—8o. A mixture of the corresponding 2-(2-arylethenyl)-1-methylbenzimidazole (6.12 mmol) or 2-(2-arylethynyl)-1-methylbenzimidazole (3.05 mmol) and 2-iodoethanol (12.24 mmol) was dissolved in toluene (15 mL) and then heated under reflux for 5 h. The precipitate was collected, washed with diethyl ether (3 × 10 mL), and dried under vacuo.

1-(2-Hydroxyethyl)-3-methyl-2-(2′-phenylethenyl)benzimidazolinium Iodide (4o). Compound **4o** was obtained as colorless needles (51%). Mp: 179 °C (acetone). ^{1}H NMR (250 MHz, DMSO-d_6), δ: 8.04−7.45 (m, 11H), 5.14 (t, $J = 6.1$ Hz, 1H), 4.71 (t, $J = 5.5$ Hz, 2H), 4.17 (s, 3H), 3.85 (m, 2H). ^{13}C NMR (63 MHz, DMSO-d_6), δ: 148.9, 146.8, 134.7, 132.6, 131.6, 131.4, 129.4, 128.8, 126.7, 113.8, 113.9, 108.8, 59.4, 48.5, 33.8. MS (EI), *m*/*z* (relative intensity): 278 (M^+, 100), 248 (23), 170 (23), 158 (50). Anal. Calcd for $C_{18}H_{19}N_2OI$: C, 53.22; H, 4.71. Found: C, 52.95; H, 4.99.

1-(2-Hydroxyethyl)-2-(2-(4″-*N*,*N*-dimethylaminophenyl)-ethenyl)-3-methylbenzimidazolinium Iodide (5o). Compound **5o** was obtained as yellowish powder (85%). Mp: 145 °C (acetone). ^{1}H NMR (250 MHz, DMSO-d_6), δ: 8.00 (d, $J =$ 16.5 Hz, 1H), 7.98 (m, 1H), 7.81−7.61 (m, 3H), 7.74 (d, $J =$ 8.2 Hz, 2H), 7.19 (d, $J = 16.5$ Hz, 1H), 6.80 (d, $J = 8.2$ Hz, 2H), 5.20 (t, $J = 5.8$ Hz, 1H), 4.66 (t, $J = 5.5$ Hz, 2H), 4.13 (s, 3H), 3.86 (m, 2H), 3.04 (s, 6H). ^{13}C NMR (63 MHz, DMSO-d_6), δ: 152.2, 149.4, 146.9, 132.3, 131.3, 130.4 (2C), 121.7, 115.9, 113.0, 112.6, 111.6, 100.9, 59.0, 47.8, 41.0, 34.7. MS (EI), *m*/*z* (relative intensity): 321 (M^+, 100), 291 (16), 214 (23), 168 (42). Anal. Calcd for $C_{20}H_{24}N_3OI$: C, 53.46; H, 5.38. Found: C, 52.99; H, 5.29.

1-(2-Hydroxyethyl)-2-(2-(4″-*N*,*N*-dimethylaminonaphthyl-)ethenyl)-3-methylbenzimidazolinium Iodide (6o). Compound **6o** was obtained as orange powder (71%). Mp: 185 °C (Acetone). ^{1}H NMR (250 MHz, DMSO-d_6), δ: 8.73 (d, J = 15.5 Hz, 1H), 8.40−8.29 (m, 2H), 7.81 (m, 1H), 7.79 (d, J = 8.1 Hz, 1H), 7.57−7.53 (m, 2H), 7.33−7.30 (m, 3H), 7.12 (d, J = 8.1 Hz, 1H), 7.11 (d, J = 16.5 Hz, 1H), 5.22 (t, J = 5.9 Hz, 1H), 4.67 (t, J = 5.5 Hz, 2H), 4.11 (s, 3H), 3.89 (m, 2H), 2.96 (s, 6H). ^{13}C NMR (63 MHz, DMSO-d_6), δ: 152.2, 149.4, 146.9, 135.6, 134.6, 132.7, 128.6, 128.2, 126.4, 125.3, 124.9, 124.5, 124.4, 122.6, 122.5, 119.3, 114.1, 113.6, 109.1, 59.4, 49.8, 45.1, 30.7. MS (EI), *m*/*z* (relative intensity): 371 (M^+, 100), 341 (37), 264 (19), 218 (35). Anal. Calcd for $C_{24}H_{26}N_3$-OI: C, 57.72; H, 5.25. Found: C, 57.19; H, 5.04.

1-(2-Hydroxyethyl)-3-methyl-2-(2′-phenylethynyl)benzimidazolinium Iodide (7o). Compound **7o** was obtained as colorless needles (62%). Mp: 139 °C (acetone). ^{1}H NMR (250 MHz, DMSO-d_6), δ: 8.13−7.59 (m, 10H), 5.10 (t, J = 5.8 Hz, 1H), 4.76 (t, J = 5.5 Hz, 2H), 4.22 (s, 3H), 3.91 (m, 2H). ^{13}C NMR (63 MHz, DMSO-d_6), δ: 139.6, 133.0, 132.3, 131.6, 131.1, 129.2, 127.3, 117.9, 113.5, 113.8, 107.8, 71.5, 58.9, 49.9, 33.3. MS (EI), *m*/*z* (relative intensity): 276 (M^+, 100), 246 (29), 170 (29), 158 (41). Anal. Calcd for $C_{18}H_{17}N_2OI$: C, 53.48; H, 4.24. Found: C, 53.15; H, 4.49.

1-(2-Hydroxyethyl)-2-(2-(4″-*N*,*N*-diethylaminophenyl)ethynyl)-3-methylbenzimidazolinium Iodide (8o). Compound **8o** was obtained as an orange powder (85%). Mp: 155 °C (acetone). ^{1}H NMR (250 MHz, DMSO-d_6) δ: 7.95−7.86 (m, 2H), 7.65−7.50 (m, 2H), 7.59 (d, J = 9.2 Hz, 2H), 6.73 (d, J = 9.2 Hz, 2H), 5.02 (t, J = 5.9 Hz, 1H), 4.62 (t, J = 5.5 Hz, 2H), 4.09 (s, 3H), 4,10−3.92 (m, 4H), 3.59 (m, 2H), 1.15 (t, J = 7.5 Hz, 6H). ^{13}C NMR (63 MHz, DMSO-d_6), δ: 148.6, 139.5, 133.4, 130.0, 125.2, 119.8, 118.3, 117.4, 115.6, 111.8, 111.2, 109.7, 99.9, 57.6, 48.1, 42.6, 31.3, 10.8. MS (EI), *m*/*z* (relative intensity): 347 (M^+, 100), 317 (45), 242 (33), 192 (37). Anal. Calcd for $C_{22}H_{26}N_3OI$: C, 55.59; H, 5.51. Found: C, 55.37; H, 5.06.

General Procedure for the Preparation of 10-(2-Arylethenyl)-9-methylbenzimidazolo[2,3-*b*]oxazolidines 4—6c. The corresponding benzimidazolinium iodide (4.5 mmol) was dissolved in freshly distilled dry THF (20 mL) and cooled to 0 °C. 7 amounts of sodium hydride (pur. 95%) were added by portion over 1 h, the reaction mixture was heated under reflux for 2 additional hours. After cooling, the mixture was concentrated under vacuo and the residue was purified by column chromatography, (SiO_2, DCM/EtOAc 1:1).

9-Methyl-10-(2-phenylethenyl)benzimidazolo[2,3-*b*]oxazolidine (4c). Compound **4c** was obtained as colorless crystals (45%). Mp: 69 °C (acetone). ^{1}H NMR (300 MHz, $CDCl_3$) δ: ^{1}H NMR (300 MHz, $CDCl_3$): 7.37 (d, J = 15.3 Hz, 1H), 7.29 (m, 2H), 7.25 (m, 2H), 7.15−7.05 (m, 5H), 6.33 (d, J = 15.3 Hz, 1H), 3.85−3.75 (m, 4H), 2.79 (s, 3H). ^{13}C NMR (63 MHz, $CDCl_3$) δ: 150.4, 149.6, 139.1, 137.3, 133.4, 128.6, 127.8, 127.0, 125.3, 122.4, 121.8, 119.3, 114.3, 110.2, 61.5, 45.9, 30.7. MS (EI), *m*/*z* (relative intensity): 278 (M^+, 35), 248 (17), 170 (100), 158 (64). MS (FAB) (*m*/*z*): 279 $[M + H]^+$. Anal. Calcd for $C_{18}H_{18}N_2O$: C, 77.67; H 6.52; Found: C, 77.63; H 6.74.

9-Methyl-10-[2-(4′-*N*,*N*-dimethylamino)phenylethenyl]benzimidazolo[2,3-*b*]oxazolidine (5c). Compound **5c** was obtained as a colorless powder (39%). Mp: 77 °C. ^{1}H NMR (300 MHz, $CDCl_3$): δ 7.58 (d, J = 15.4 Hz, 1H), 7.29 (m, 2H), 7.19 (d, J = 8.7 Hz, 2H), 7.04 (m, 2H), 6.72 (m, 2H), 6.58 (d, J = 8.7 Hz, 2H), 6.05 (d, J = 15.4 Hz, 1H), 3.85−3.75 (m, 4H), 2.95 (s, 6H), 2.83 (s, 3H). ^{13}C NMR (63 MHz, $CDCl_3$) δ: 151.7, 149.8, 139.1, 133.4, 127.7, 127.1, 124.2, 122.4, 121.8, 120.3, 114.7, 112.9, 110.7, 63.4, 47.8, 40.5, 30.7. MS (EI), *m*/*z* (relative intensity): 321 (M^+, 40), 291 (12), 214 (100), 168 (60). MS (FAB) (*m*/*z*): 322 $[M + H]^+$. Anal. Calcd for $C_{20}H_{23}N_3O$: C, 74.74; H, 7.21. Found: C, 74.47; H, 7.29.

10-[2-(4′-*N*,*N*-Dimethylamino)naphthylethenyl]-9-methylbenzimidazolo[2,3-*b*]oxazolidine (6c). Compound **6c** was obtained as a powder (21%). Mp: 83 °C (petroleum ether). ^{1}H NMR (300 MHz, $CDCl_3$): δ 8.48 (d, J = 18.3 Hz, 1H), 8.17 (m, 2H), 7.49 (m, 2H), 7.31 (m, 2H), 7.08 (d, J = 7.7 Hz, 1H), 6.92 (d, J = 7.7 Hz, 1H), 6.71 (m, 2H), 6.27 (d, J = 18.3 Hz, 2H), 3.85−3.75 (m, 4H), 2.91 (s, 6H), 2.87 (s, 3H). ^{13}C NMR (63 MHz, $CDCl_3$) δ: 151.3, 149.6, 139.4, 133.4, 131.2, 128.7, 127.5, 127.3, 126.5, 125.4, 124.8, 122.4, 121.2, 119.3, 114.5, 112.9, 111.5, 63.8, 47.1, 40.4, 30.2. MS (EI), *m*/*z* (relative intensity): 371 (M^+, 35), 341 (13), 264 (100), 218 (45); MS (FAB), *m*/*z*: 372 $[M + H]^+$. Anal. Calcd for $C_{24}H_{25}N_3O$: C, 77.60; H, 6.78. Found: C, 77.49; H, 6.67.

Acknowledgment. Corning-CERF (Fontainebleau, France) is greatly acknowledged for its financial support. V.R. is indebted to the Région Aquitaine for financial support in optical, laser, and computer equipment. M.G. and B.C. thank the Belgian Federal Science Policy (IUAP No. P5-03 "Supramolecular Chemistry and Supramolecular Catalysis") for financial support. B.C. thanks the Belgian National Fund for Scientific Research (FNRS) for his research director position. This work has benefited from a scientific cooperation established and supported by the Centre National de la Recherche Scientifique (CNRS), the FNRS, and the Commissariat Général aux Relations Internationales (CGRI) de la Communauté Wallonie-Bruxelles. The calculations were performed thanks to computing time made available by the SiMoA (Simulation et Modélisation en Aquitaine, France), the intensive calculation pole "M3PEC-MESOCENTRE" of the University Bordeaux I, as well as by the Interuniversity Scientific Computing Facility (ISCF), installed at the Facultés Universitaires Notre-Dame de la Paix (Namur, Belgium), for which the authors gratefully acknowledge the financial support of the FNRS−FRFC and the "Loterie Nationale" for the Convention no. 2.4578.02 and the financial support of the FUNDP.

References and Notes

(1) (a) *Molecular Switches*; Feringa, B. L., Ed.; Wiley-VCH: Weinheim, Germany, 2001. (b) Lucas, L.; De Jong, J.; Van Esch, J.; Kellogg, R. M.; Feringa, B. L. *Eur. J. Org. Chem.* **2003**, *1*, 155.

(2) Delaire, J. A.; Nakatani, K. *Chem. Rev.* **2000**, *100*, 1817.

(3) (a) Atassi, Y.; Delaire, J. A.; Nakatani, K. *J. Phys. Chem. Rev.* **1995**, *99*, 16320. (b) Barachevsky, V.; Chudinova, G. *Mol. Sci. Eng. C* **1999**, *8*−*9*, 73.

(4) (a) Pina, F.; Melo, M. J.; Maestri, M.; Ballardini, R.; Balzani, V. *J. Am. Chem. Soc.* **1997**, *119*, 5556. (b) *Organic Photochromic and Thermochromic Compounds*, Crano, J. C., Guglielmetti, R. J., Eds.; Plenum Press: New York, 1999; Vol. 1. (c) Bouas-Laurent, H.; Dürr, H. *Pure Appl. Chem.* **2001**, *73*, 639.

(5) Sanguinet, L.; Pozzo, J. L.; Rodriguez, V.; Adamietz, F.; Castet, F.; Ducasse, L.; Champagne, B. *J. Phys. Chem. B* **2005**, *109*, 11139.

(6) (a) Wortmann, R.; Krämer, P.; Glania, C.; Lebus, S.; Detzer, N. *Chem. Phys. Lett.* **1993**, *173*, 99. (b) Meyers, F.; Marder, S.; Pierce, B. M.; Brédas, J. L. *J. Am. Chem. Soc.* **1994**, *116*, 10703. (c) Verbiest, T.; Houbrechts, S.; Kauranen, M.; Clays, K.; Persoons, A. *J. Mater. Chem.* **1997**, *7*, 2175. (d) Raimundo, J. M.; Blanchard, P.; Gallego-Planas, N.; Mercier, N.; Ledoux-Rak, I.; Hierle, R.; Roncali, J. *J. Org. Chem.* **2002**, *67*, 205. (e) Cho, M.; Am, S. Y.; Lee, H.; Ledoux, I.; Zyss, J. *J. Chem. Phys.* **2002**, *116*, 9165. (f) Brunel, J.; Mongin, O.; Jutand, A.; Ledoux, I.; Zyss, J.; Blanchard-Desce, M. *Chem. Mater.* **2003**, *15*, 4139. (g) Champagne, B.; André, J. M.; Botek, E.; Licandro, E.; Maiorana, S.; Bossi, A.; Clays, K.; Persoons, A. *ChemPhysChem* **2004**, *5*, 1438. (h) Frediani, L.; Ågren, H.; Ferrighi, L.; Ruud, K. *J. Chem. Phys.* **2005**, *123*, 144117. (i)

Chen, W.; Li, Z. R.; Wu, D.; Li, Li, Y.; Sun, C. C.; Gu, F. L. *J. Am. Chem. Soc.* **2005**, *127*, 10977. (j) Maury, O.; Le Bozec, H. *Acc. Chem. Res.* **2005**, *38*, 691.

(7) (a) Clays, K.; Persoons, A.; De Maeyer, L. *Adv. Chem. Phys.* **1994**, *85*, 455. (b) Hendrickx, E.; Clays, K.; Persoons, A. *Acc. Chem. Res.* **1998**, *31*, 675.

(8) (a) Kanis, D. R.; Ratner, M. A.; Marks, T. J. *Chem. Rev.* **1994**, *94*, 195. (b) Champagne, B.; Kirtman, B. In *Handbook of Advanced Electronic and Photonic Materials and Devices*; Nalwa, H. S., Ed.; Academic Press: New York, 2001, Vol. 9, Chapter 2, p 63.

(9) Bersohn, R.; Pao, Y. H.; Frisch, H. L. *J. Chem. Phys.* **1966**, *45*, 3184.

(10) Frisch, M. J.; Trucks, G. W.; Schlegel, H. B.; Scuseria, G. E.; Robb, M. A.; Cheeseman, J. R.; Montgomery, J. A., Jr.; Vreven, T.; Kudin, K. N.; Burant, J. C.; Millam, J. M.; Iyengar, S. S.; Tomasi, J.; Barone, V.; Mennucci, B.; Cossi, M.; Scalmani, G.; Rega, N.; Petersson, G. A.; Nakatsuji, H.; Hada, M.; Ehara, M.; Toyota, K.; Fukuda, R.; Hasegawa, J.; Ishida, M.; Nakajima, T.; Honda, Y.; Kitao, O.; Nakai, H.; Klene, M.; Li, X.; Knox, J. E.; Hratchian, H. P.; Cross, J. B.; Adamo, C.; Jaramillo, J.; Gomperts, R.; Stratmann, R. E.; Yazyev, O.; Austin, A. J.; Cammi, R.; Pomelli, C.; Ochterski, J. W.; Ayala, P. Y.; Morokuma, K.; Voth, G. A.; Salvador, P.; Dannenberg, J. J.; Zakrzewski, V. G.; Dapprich, S.; Daniels, A. D.; Strain, M. C.; Farkas, O.; Malick, D. K.; Rabuck, A. D.; Raghavachari, K.; Foresman, J. B.; Ortiz, J. V.; Cui, Q.; Baboul, A. G.; Clifford, S.; Cioslowski, J.; Stefanov, B. B.; Liu, G.; Liashenko, A.; Piskorz, P.; Komaromi, I.; Martin, R. L.; Fox, D. J.; Keith, T.; Al-Laham, M. A.; Peng, C. Y.; Nanayakkara, A.; Challacombe, M.; Gill, P. M. W.; Johnson, B.; Chen, W.; Wong, M. W.; Gonzalez, C.; Pople, J. A.; GAUSSIAN 03, Revision C.02, Gaussian, Inc., Pittsburgh, PA, 2003.

(11) (a) Ridley, J. E.; Zerner, M. C. *Theor. Chim. Acta* **1973**, *32*, 111. (b) Ridley, J. E.; Zerner, M. C. *Theor. Chim. Acta* **1976**, *42*, 223. (c) Bacon, A. D.; Zerner, M. C. *Theor. Chim. Acta* **1979**, *53*, 21. (d) Zerner, M. C.; Loew, G. H.; Kirchner, R. F.; Mueller-Westerhoff, U. T. *J. Am. Chem. Soc.* **1980**, *102*, 589.

(12) MOS−F (Semiempirical Molecular Orbital package for Spectroscopy), Fujitsu V4.

(13) (a) Zerner, M. C. In *Reviews of Computational Chemistry*; Lipkowitz, K. B., Boyd, D. B., Eds.; VCH: New York, 1991; Vol. 1, p 313. (b) Martin, C. H.; Zerner, M. C. In *Inorganic Electronic Structure and Spectroscopy*; Solomon, E. I., Lever, A. B. P., Eds.; Wiley: New York, 1999; Vol. 1, p 555.

(14) See for example, in the case of second-order NLO responses: (a) Meyers, F.; Brédas, J. L.; Zyss, J. *J. Am. Chem. Soc.* **1992**, *114*, 2914. (b) Dehu, C.; Meyers, F.; Hendrickx, E.; Clays, K.; Persoons, A.; Marder, S. R.; Brédas, J. L. *J. Am. Chem. Soc.* **1995**, *117*, 10127.

(15) See for example, (a) Morley, J. O. *J. Chem. Soc., Faraday Trans.* **1991**, *87*, 3009. (b) Morley, J. O. *J. Phys. Chem.* **1995**, *99*, 10166.

(16) See for example (a) Kanis, D. R.; Ratner, M. A.; Marks, T. J.; Zerner, M. C. *Chem. Mater.* **1991**, *3*, 19. (b) Albert, I. D. L.; Marks, T. J.; Ratner, M. A. *J. Phys. Chem.* **1996**, *100*, 9714.

(17) (a) Sekino, H.; Bartlett, R. J. *J. Chem. Phys.* **1986**, *85*, 976. (b) Karna, S. P.; Dupuis, M. *J. Comput. Chem.* **1991**, *12*, 487.

(18) Dewar, M. J. S.; Zoebisch, E. G.; Healy, E. F.; Stewart, J. J. P. *J. Am. Chem. Soc.* **1985**, *107*, 3902.

(19) Stewart, J. J. P. *J. Comput. Chem.* **1989**, *10*, 209.

(20) Stewart, J. J. P. *J. Mol. Mod.* **2004**, *10*, 6.

(21) (a) Castet, F.; Champagne, B. *J. Phys. Chem. A* **2001**, *105*, 1366. (b) Botek, E.; Champagne, B. *J. Appl. Phys. B* **2002**, *74*, 627. (c) Guillaume, M.; Botek, E.; Champagne, B.; Castet, F.; Ducasse, L. *J. Chem. Phys.* **2005**, *121*, 7390.

(22) MOPAC2000, Fujitsu Limited, 1999; Stewart, J. J. P. Quantum Chemistry Program Exchange, no. 455.

(23) Cohen, H. D.; Roothaan, C. C. J. *J. Chem. Phys.* **1965**, *43*, S34.

(24) Davis, P. J.; Rabinowitz, P. In *Numerical Integration*; Blaisdell Publishing Company: London, 1967, p 166.

(25) (a) Rice, M. J.; Handy, N. *Int. J. Quantum Chem.* **1992**, *43*, 91. (b) Sekino, H.; Bartlett, R. J. *Chem. Phys. Lett.* **1995**, *234*, 87. (c) Jacquemin, D.; Champagne, B.; Hättig, C. *Chem. Phys. Lett.* **2000**, *319*, 327.

(26) Bulat, F. A.; Toro-Labbé, A.; Champagne, B.; Kirtman, B.; Yang, W. *J. Chem. Phys.* **2005**, *123*, 014319.

(27) Willetts, A.; Rice, J. E.; Burland, D. A.; Shelton, D. P. *J. Chem. Phys.* **1992**, *97*, 7590.

(28) Bersohn, R.; Pao, Y. H.; Frisch, H. L. *J. Chem. Phys.* **1966**, *45*, 3184.

(29) Würthner, F.; Yao, S.; Debaerdemaeker, T.; Wortmann, R. *J. Am. Chem. Soc.* **2002**, *124*, 9431.